THE LHCB RING IMAGING CHERENKOV DETECTORS

STEPHAN EISENHARDT
University of Edinburgh, Dept. of Physics and Astronomy, Mayfield Road, Edinburgh EH9 3JZ, UK

LHCb is an experiment for precise measurements of CP-violation in the decays of B mesons. Very good charged particle identification will be crucial for clean measurements of rare CP violating decays against an abundant background as well as for efficient kaon tagging. Thus LHCb employs two Ring Imaging Cherenkov (RICH) detectors to achieve K-π separation over a wide range of momenta. This paper presents the status of the LHCb RICH project. The requirements and the design of the detector are covered. The choices of the radiators and on R&D results for the photodetectors are reported. And the adopted solutions for the sub-components of the detector are discussed. Finally, the expected performance of the RICH detectors projected from full scale simulation based on R&D results is shown.

1 Introduction

The LHCb experiment will exploit the large rate of B mesons which will be provided in pp-collisions of the Large Hadron Collider (LHC) when it becomes operational in 2006. LHCb is designed to precisely measure the observables of CP-violation in the decays of B mesons. Excellent particle identification is a fundamental requirement of the LHCb experiment as meaningful CP-violation measurements are only possible in many important channels if hadron identification, and most importantly the distinction between pions and kaons, is available.

The LHCb detector is laid out as a forward single-arm spectrometer with an acceptance of $10\dots300\,\text{mrad}^a$ ($10\dots250\,\text{mrad}$) in the (non-)bending plane catching most of the B mesons emitted into one hemisphere. The particle identification is achieved using Ring-Imaging Cherenkov (RICH) detectors [1]. Their placement within the LHCb spectrometer can be seen in Fig. 1, which shows the top view of the experiment.

2 The RICH Project

2.1 Requirements and Design

The momentum range in which excellent particle identification is required can be seen from Fig. 2. The highest particle momenta are reached in the two-body decay $B_d \to \pi\pi$ where the tail of the distribution exceeds 150 GeV. On the other end the momentum range are kaons, used for tagging the b flavor,

[a]Equivalent to $\eta \approx 1.89\ldots \approx 5.30$ in units of pseudo rapidity.

which can have momenta as low as 1 GeV. Particle identification in such a wide range is only achievable with RICH detectors using several radiators. Table 1a) gives the thresholds of momenta for π an K mesons for the three radiators chosen for the LHCb RICH system. The distribution of polar angles Θ versus particle momenta, shown in Fig. 3, demonstrates how the phase space can be covered by the use of two distinct subsystems. RICH 1 is sensitive to the full angular acceptance but is limited to the low momentum region. RICH 2 operates over the full momentum range but is restricted to a smaller angular region.

a)	Aerogel	C_4F_{10}	CF_4	
π	0.6	2.6	4.4	GeV
K	2.0	9.3	15.6	GeV

b)	Aerogel	C_4F_{10}	CF_4	
n_{ph}	7	33	18	
$\delta\Theta_C$	2.00	1.45	0.58	mrad

Table 1. Radiators used by LHCb RICH: a) radiator thresholds for mesons; b) number of detected photons n_{ph} and angular resolution $\delta\Theta_C$ as determined from simulation.

The detector design chosen by LHCb can be seen in Fig. 4. The angular acceptances in the bending plane are 300 mrad for RICH 1 and 120 mrad for RICH 2, respectively. Spherical mirrors are used to focus the Cherenkov photons emitted by charged particles traversing the radiators with a momentum above the threshold to ring images on the photodetector plane. The spherical mirrors are tilted with respect to the beam axis to position the photodetector arrays outside the acceptance of subsequent detector systems. In RICH 2 a second set of planar mirrors is placed in the detection volume outside the RICH 2 acceptance to shorten the overall length of the detector. RICH 1 uses a 5 cm-thick aerogel radiator and a 85 cm-long C_4F_{10} gas radiator. The CF_4 gas radiator in RICH 2 has an approximate length of 170 cm.

A particular challenge of the LHCb RICH project are the photodetectors. A sensitive area of $2.6\,m^2$ has to be covered with a pixel granularity of $\sim 2.5 \times 2.5\,mm^2$ and a large active area fraction of $\geq 73\,\%$. The pixels have to be sensitive to single photons in the wavelength range $200 \ldots 600\,nm$ with a quantum efficiency $> 20\,\%$. These requirements lead to about 310.000 electronic channels which have to be read out at the LHC speed of $40\,MHz$. In addition, the photodetectors have to sustain the LHCb environment with residual magnetic fields and charged particles traversing the photodetectors and have to be radiation tolerant.

2.2 Photodetectors

Hybrid Photodiodes (HPD) have been adopted as the baseline solution for the RICH photodetectors. The status of their R&D is summarized in a contribution to this conference [2]. Multianode photomultiplier tubes (MaPMT) have been chosen as backup photodetectors. MaPMT are commercially available and have been slightly modified to suit the requirements of LHCb RICH[b]. With an anode and dynode chain segmented into an array of 8×8 channels of $2.3 \times 2.3\,mm^2$ in one housing of $1''$ square they provide the highest possible density of photomultiplier channels available. The bialkali photocathode provides a quantum efficiency of 25 % at $\lambda = 380\,nm$. In an R&D project this technology has been shown to meet the LHCb requirements. A 3×3 cluster prototype of close-packed MaPMT was equipped with quartz glass lenses which focused the incident light on the active area of the MaPMTs in order to recover the inactive area caused by the MaPMT housing. This increased the effective pixel size to $3.2 \times 3.2\,mm^2$ at the surface of the lens while increasing the active area fraction from 38 % to 85 % with the remaining inefficiency due to the $0.2\,mm$ separation of the pixels within one tube. The performance of this prototype cluster mounted onto a RICH 1 prototype was studied with the CERN SPS test beam using 120 GeV pions[3]. The MaPMT were read out at the LHCb data acquisition speed of 40 MHz using APVm chips. Fig. 5 shows the recorded photons from 6000 events after subtraction of all experimental effects. A Cherenkov ring is clearly visible and the observed photon yield ($6.51 \pm 0.34\,ph.e.$) is in very good agreement with the simulation ($6.21\,ph.e.$).

2.3 Construction of Subsystems

Fig. 6 displays half a frame of the RICH 1. Charged particles from the interaction point will traverse the low mass window of the vertex tank, the kapton seal of the RICH 1 volume, the aerogel and the gas radiator volume, the spherical mirrors and finally the exit kapton seal. With that the material budget of the RICH 1 amounts to 14 % of a radiation length X_0.

The low mass exit window of the vertex tank forms one unit with the LHC beampipe running through RICH 1 and is mechanically very delicate at the connection of the two parts due to the long lever arm of the beampipe. Special provisions have been designed and simulated to ensure stress-free mounts in production, transport and installation, with the last the most critical process. The flange of the window finally will be fixed to the RICH 1 frame, while the beampipe will be supported from the RICH 1 frame by steel wires.

The kapton seals act as windows of the RICH 1 gas radiator volume and are glued directly to the LHCb beampipe. They consist of three layers with a radial slit each, rotated by $120\,^\circ$, to mount them in-situ to a gas tight fit with the beampipe installed. The kapton foils are radially corrugated for pressure tolerance. A prototype has successfully proven the feasibility of this approach.

[b] A UV-glass window instead of the standard borosilicate window and the 1-mm production rim removed for close packing.

The RICH 1 mirror mounts consist of 3-leg spiders made of carbon fiber using plastic screws to adjust the four mirror segments per quadrant to better than 0.1 mrad. A prototype mount has proven to provide 0.01 mrad precision with a very good repeatability and log-term stability under the load expected for the 6 mm-thick glass mirrors. Ongoing studies investigate alternatives to the glass mirrors which contribute 4.5 % of a radiation length to the material budget of RICH 1. Beryllium mirrors of 5 mm thickness would contribute 2 % instead and are likely to replace the glass mirrors as the baseline technology. Composite mirrors using an aramid phenolic honeycomb or foamed moulded glass as a core between layers of carbon fiber and a perspex mirror only would contribute 1 % but pose technical challenges not yet solved.

A hygroscopic variant of aerogel has been adopted as the radiator material in RICH 1. With a refractive index of $n = 1.034$, clarity of $0.00045 \mu m^4/cm^{-1}$ and no degradation due to radiation in the lifetime of LHCb it provides the best overall solution. The thickness of the radiator is a trade-off between the yield of Cherenkov photons, the fraction of Rayleigh scattered photons and the amount of radiation length. It was chosen to be 5 cm.

Fig. 7 shows the design of the RICH 2 frame with the low mass windows for the particle entry in the front and the exit in the back. In the center a beam pipe envelope connects the windows and acts as center gas seal. In the detector volume the planes supporting the spherical mirrors and the planar mirrors are visible. The material budget of the RICH 2 amounts to 12.4 % X_0. Left and right to the detector volume the photodetector arrays are mounted in housings of soft iron, weighing 4 tons each, acting as global magnetic shield. In addition the photodetectors need to be shielded individually to cope with the magnetic stray fields of ~ 150 Gauss at the location of the photodetector housings.

Finite element analyses have been performed to optimize the design of the RICH 2 frame under load and for natural frequencies. The study showed that even with magnetic shields weighing 2×11000 kg maximum deflections of <5 mm can be achieved. With the same design a fundamental eigen frequency of ~ 6 Hz is achieved.

The entry and exit window have to be low mass but also have to be stiff enough to only yield low deflections under pressure despite of their size. A sandwich of two 1 mm fiber skins with a 48 mm polymethacrylimide (PMI) foam core behaves optimal with respect to the window deflection and mass requirements. At an under- or overpressure of 400 Pa the maximum deflection is ~ 30 mm. Such a pressure difference then imposes a stress of ~ 1 ton on the beampipe envelope. Thus, careful optimization of the flanges connecting the envelope to the windows has been done for material budget and the stress minimization using finite element analysis.

The quartz glass windows sealing the RICH 2 gas volume against the photodetectors are with 1500×750×5 mm to big to be cut form one standard sized production pane. Therefore a window frame has been designed for two window segments connected by a few-mm slim gas tight joint. The transmission characteristics of he quartz glass is with 90 % transmission for $\lambda > 190\,\mathrm{nm}$ better than required.

Tools will be developed to monitor the photodetectors while commissioning the detector and within normal operation. Using LED or laser light injected via fibers and reference detectors a fast debugging system is intended to be used to investigate magnetic field distortions present in the photodetectors, to monitor the photodetector functionality, the aging and the mirror reflectivities and to support the mirror alignment.

2.4 Physics

Using a full simulation of the LHCb detector, based on global pattern recognition and including all background processes a detailed comparison of the RICH performance for the different photodetector options was carried out based on measured test beam data. The results for HPDs and MaPMTs are very similar. Here the results of the HPDs are reported. Fig. 8 shows the π-K separation for particles stemming from $B_d \rightarrow \pi\pi$ decays in units of standard deviation versus the particle momentum. Indicated is in which regions the different radiators predominantly contribute. In the region of $3\ldots85$ GeV in average a π-K separation of better than $3\,\sigma$ is achieved. At higher momentum the separation levels off at $2\,\sigma$ and is still good enough to significantly enhance the purity of the data samples. The number of detected photons n_{ph} and the angular resolution $\delta\Theta_C$ expected using the three radiators are given in table 1b).

The LHCb experiment has the unique feature to over constrain the angles of the Unitarity Triangles in the Wolfenstein approximation which are labelled α, β, γ and $\delta\gamma$ by measuring many CP-violating asymmetries in a single experiment. Thus, new strategies can be used, e.g. the combination of $B_s \rightarrow KK$ and $B_d \rightarrow \pi\pi$ allows to measure γ to $\sigma_\gamma \sim 4^\circ$ with data from one year. Fig. 9 displays the signal-to-background ratio for the $B_s \rightarrow KK$ channel without and with the particle identification provided by the RICH giving a very clean sample in the second case. Similarly, the channel $B_d \rightarrow \pi\pi$, which is sensitive to α, benefits from the reduction of background from $B_d \rightarrow K\pi$ which could be partially CP-violating, giving $\sigma_\alpha \sim 2\ldots5^\circ$ provided the fraction of Penguin contribution is determined from elsewhere, e.g. from the process $B_d \rightarrow \rho\pi$. And finally the RICH detector allows to separate channels with large track multiplicity like $B_s \rightarrow D_s^{\mp}K^{\pm}$ from the much more prevalent background $B_s \rightarrow D_s\pi^+$. This allows the measurement of $\gamma - \delta\gamma$ to $6 \ldots 14°$ with only 2400 events in one year.

3 Conclusions

The RICH detector is essential for the physics programme of the LHCb experiment by providing charged particle identification which is necessary for precise measurements of CP-violation. The physics performance studies have been extended since the Technical Proposal for a more complete picture. The RICH project is progressing since the Technical Design report and the design for the subsystems are detailed and advanced. The project is in the transition from R&D to construction and is still on track to take data when the LHC becomes operational in 2006.

Acknowledgments

I am grateful to the members of the LHCb RICH group for their support when preparing this paper.

References

1. *LHCb - RICH Technical Design Report.* By LHCb Collaboration (S. Amato, et al.), CERN/LHCC/2000-0037, LHCb TDR 3, Sep 2000.
2. *The pixel hybrid photodetectors for the LHCb-RICH counters.* Maria Girone, in *these proceedings.*
3. *Performance of a Cluster of Multi-anode Photomultipliers Equipped with Lenses for use in a Prototype RICH Detector.* V. Gibson, et al., LHCb-2001-091 RICH, 18th June 2001. Submitted to Nucl. Instrum. Methods

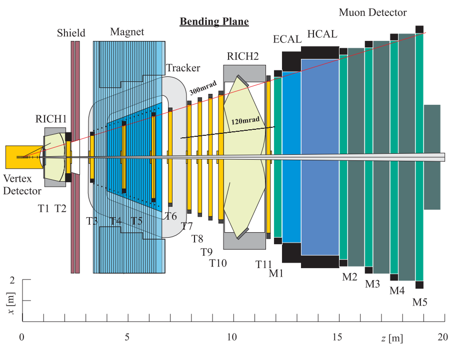

Figure 1. Top view on the LHCb detector (bending plane).

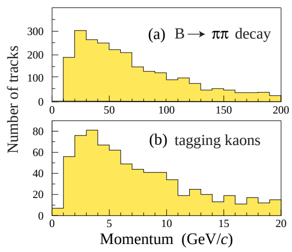

Figure 2. Momentum distribution of decay products: a) from $B_d \rightarrow \pi\pi$, b) for tagging kaons.

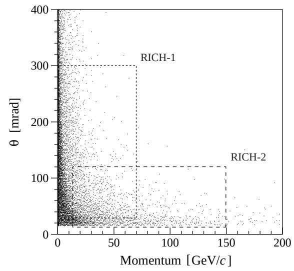

Figure 3. Polar angle Θ versus the particle momentum for all tracks in $B_d \to \pi\pi$.

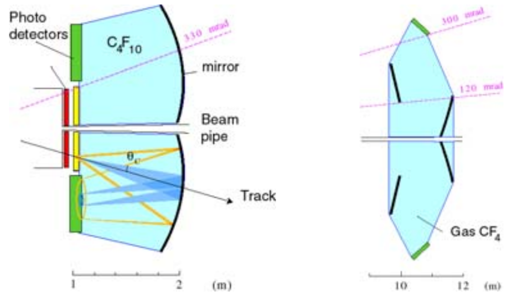

Figure 4. The LHCb RICH detectors (top view). Regard the different scales for RICH 1 and RICH 2.

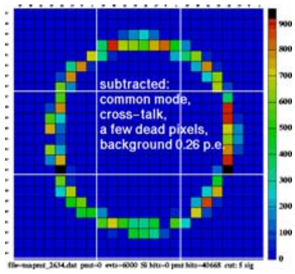

Figure 5. Cherenkov ring images (6000 events) taken with a 3 × 3 cluster of MaPMTs.

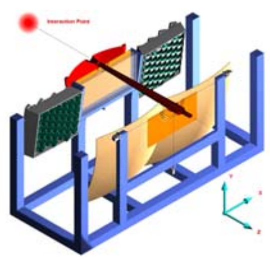

Figure 6. Half frame of RICH 1.

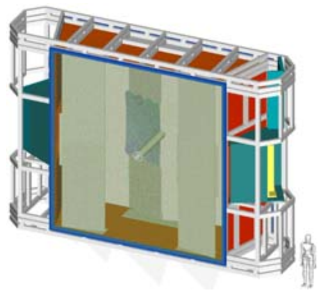

Figure 7. RICH 2 frame.

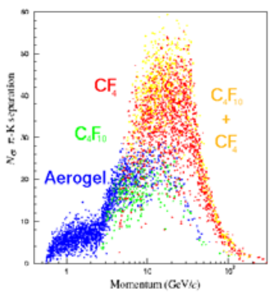

Figure 8. π-K separation versus particle momentum.

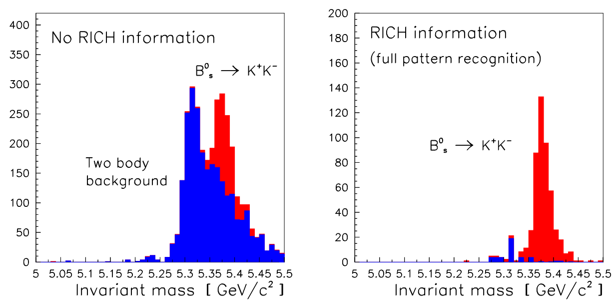

Figure 9. $B_s \to KK$ identification without and with RICH.